Int J Adv Manuf Technol (2004) 23: 874–881
DOI 10.1007/s00170-003-1736-5

ORIGINAL ARTICLE

C. H. Liu · A. Chen · Y.-T. Wang · C.-C. A. Chen

Modelling and simulation of an automatic grinding system using a hand grinder

Received: 14 November 2002 / Accepted: 11 March 2003 / Published online: 10 March 2004

Abstract A grinding process model for an automatic grinding system with grinding force control is developed in this paper. This grinding system utilises an electric hand grinder, driven by a CNC machine centre and a force sensor for force measurement. This model includes compliance of the grinding system and is initially represented by a series of springs. The stiffness of each component is estimated in this study and it is found that the model may be simplified into a single spring-mass system. A corresponding PID controller is designed for the purpose of grinding force control, which calculates the appropriate CNC spindle displacement according to the force measured by the force sensor. Computer simulation results show that the system settling time is less than 0.25 s.

Keywords Applications grinding · Grinding system simulation · Automatic grinding system

1 Introduction

It is known that force control may improve grinding results of mould and dies [1, 2, 3, 4, 5, 6], and hence force control has become an important procedure for grinding and surface finishing processes. Recently, electric hand grinders have become popular surface finishing tools of moulds and dies. They have already been included in automatic surface finishing systems [7, 8], in which hand grinders are driven by CNC machine centres. However, corresponding force control techniques for these systems have not been developed. In this study, therefore, a grinding process model for an automatic grinding system using hand grinders is proposed, and a corresponding PID controller has been designed. The system is similar to that of Chen and Duffie [7], and Hsu [8], but a force sensor is placed under the work-piece for force measurement. The system is shown in Fig. 1. The model proposed in this paper has been implemented in the grinding system [9] and grinding force control experiments have been performed.

Several grinding force models have been proposed. A good summary of these models, up to the year 1992, is given by Tönshoff et al. [10]. In these models basically normal grinding forces are related to cutting speed, various forms of working engagement and wheel diameters. Recently Ludwick et al. [11], and Jenkins and Kurfess [12] suggested the model

$$Q = K_p(F_N - F_{TH})V \tag{1}$$

where Q is material removal rate, F_N is normal force, F_{TH} is the threshold value of F_N, V is the relative speed, and K_p is a proportion constant. This model is a combination of the model proposed by Hahn and Lindsay [13], in which normal grinding force is proportional to material removal rate, and the 'Preston equation' (see [14]), which states that normal force is inversely proportional to he relative speed between wheel and work-piece. This model has been adopted by Jenkins and Kurfess [15], [5], and Hekman and Liang [16] for grinding force estimation. A similar model was suggested by Kurfess, et al. [17], Whitney et al. [18] and Kurfess and Whitney [19]. In a series of studies for weld bead grinding systems, they utilised the expression

$$Q = K_1P - K_2 \tag{2}$$

where the power P is the product of the grinding force and the relative speed.

C. H. Liu (✉) · Y.-T. Wang
Department of Mechanical Engineering, Tamkang University, Tamsui, Taipei Shien, Taiwan ROC 251
E-mail: chaohwa@mail.tku.edu.tw

A. Chen
Desktop Display Business Unit, Product Development Department, AU Optronics Corporation, 23 Li-Hsin Rd. Science-Based Industrial Park, Hsinchu 300, Taiwan ROC

C.-C. A. Chen
Department of Mechanical Engineering, National Taiwan University of Science and Technology, #43, Sec.4, Keelung Rd., Taipei, Taiwan ROC 106

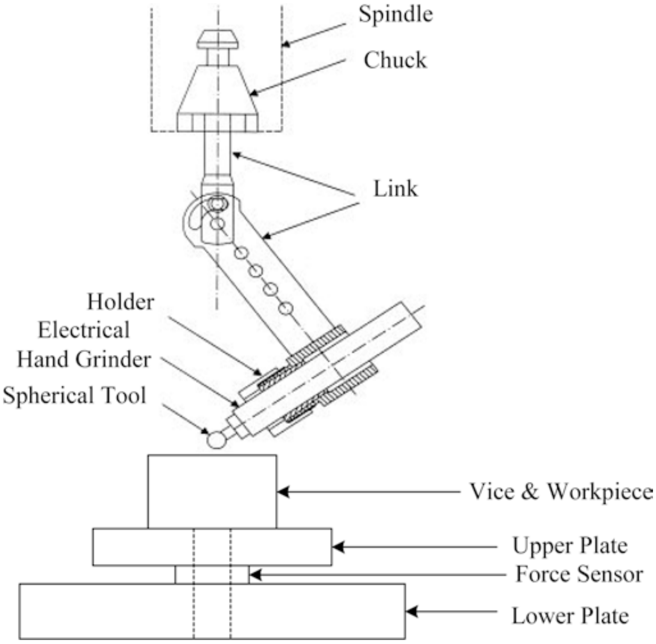

Fig. 1 Grinding system

All the models discussed above deal with grinding wheels. So far there is no process model for electric hand grinders using spherical tools. For such grinding processes, previous results [20] show that rotation speed has little contribution to grinding forces; hence velocity V in Eq. 1 is not included in the present model. Also, in all the previous models machine compliance was not considered. In this study, compliance of the grinding system shown in Fig. 1 is included in the model.

2 Grinding process model

The grinding system shown in Fig. 1 is modelled after the system shown in Fig. 2. In this figure, M and k_1 represent mass and stiffness of the electric hand grinder (including link and holder in Fig. 1) respectively, k_2 is stiffness of the material removal process, which is defined as the ratio of normal grinding force to grinding depth (assumed to be a constant). The symbols m and k_3 denote mass and stiffness of the work-piece, and k_4 is stiffness of the force sensor. Displacements x_1, x_2, x_3 and x_4 are measured from static equilibrium positions; hence gravity forces may be neglected. In Fig. 2, P is the force imposed by the CNC machine centre. Also, in the present model, the ratio of the normal grinding force to the grinding depth is assumed to take a constant value k_2, in reality, however, the relation between the grinding force and the grinding depth is expected to be nonlinear. The symbol F_d is used to represent the nonlinear term (i.e. real grinding force $= k_2x_2+F_d$).

Springs k_1, k_2, and k_3 are in series and they are equivalent to a spring with the equivalent spring constant K. Estimations of k_1, k_2, k_3 and K are shown in the

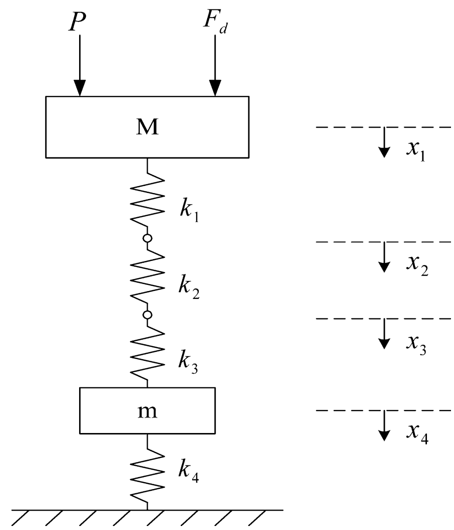

Fig. 2 Modelling of the grinding system

appendix and it is found that the equivalent spring constant K is dominated by k_2. Generally k_2 is much less than the stiffness of the force sensor k_4, hence one may expect that $k_2 \gg K$. For example, the ratio k_4/K for the current system is larger than 10^5. With this expectation (i.e. $k_4 \gg K$) in mind, it may be assumed that $k_4 \to \infty$ and $x_4 \to 0$. Then the model shown in Fig. 2 may be simplified to the one shown in Fig. 3.

Eqation of motion of the system is

$$P(t) + F_d(t) - F(t) = M\ddot{x}_1 \tag{3}$$

where

$$F(t) = Kx_1 \tag{4}$$

is the spring force. Differentiating both sides of Eq. 4, one may obtain

$$\ddot{F}(t) = K\ddot{x}_1 \tag{5}$$

Substituting Eq. 5 into Eq. 3, one gets

$$P(t) + F_d(t) - F(t) = \frac{M}{K}\ddot{F}(t) \tag{6}$$

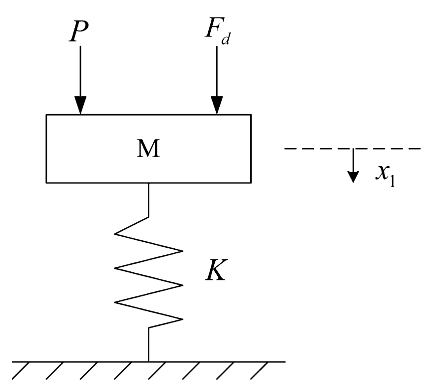

Fig. 3 Simplified model

Taking the Laplace transform for both sides of Eq. 6, also assuming zero initial conditions, one may obtain

$$P(s) + F_d(s) - F(s) = \frac{Ms^2}{K} F(s) \tag{7}$$

From this equation, the block diagram of the process model may be drawn, as shown in Fig. 4.

In this diagram, the input $P(s)$ is the force applied by CNC machine centre, the disturbance $F_d(s)$ is the non-linear grinding force defined above, the output $F(s)$ is the force measured by the force sensor. The transfer function of the block diagram is defined by $G_P(S) = F(S)/P(S)$. Using Eq. 7, also assuming $F_d(s) = 0$ one may obtain

$$G_P(S) = \frac{F(S)}{P(S)} = \frac{1}{\frac{M}{K}s^2 + 1} \tag{8}$$

3 Controller design

In this study, a PID controller is utilised and is represented as $G_c(S) = K_p + \frac{K_i}{S} + K_d S$. The block diagram

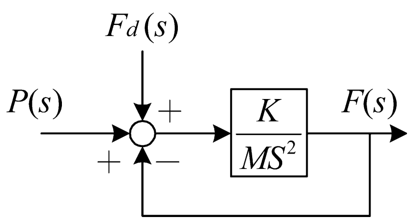

Fig. 4 Block diagram of the process

of the grinding system is shown in Fig. 5. In this figure, $F^*(S)$ is the input force command, $F(s)$ is the value measured by the force sensor, and $e(S) = F^*(s) - F(S)$ is error. In order to investigate if the system may be controlled under the steady state condition, the disturbance $F_d(s)$ is set to zero. From Fig. 5 and Eq. 8 one may show that the system transfer function $G(s)$ in Fig. 5 is given by

$$G(s) = \frac{F(s)}{F^*(s)} = \frac{K_d s^2 + K_p s + K_i}{\frac{M}{K}s^3 + K_d s^2 + (1 + K_p)s + K_i} \tag{9}$$

In steady state, $s \to 0$, from Eq. 9 it is assumed that

$$\lim_{s \to 0} \frac{F(s)}{F^*(s)} = \frac{K_i}{K_i} = 1 \tag{10}$$

This means $F(s) = F^*(s)$, hence the system may be controlled in the steady state.

Since $F(t) = Kx_1(t)$, differentiating both sides of this expression, one finds

$$\dot{F}(t) = K\dot{x}_1 = KV(t) \tag{11}$$

where $V(t)$ is velocity of the spindle. Taking the Laplace transform of this equation, one finds

$$SF(S) = KSx_1(S) = KV(S) \tag{12}$$

Hence the term $K_d SF(S)$ in Fig. 5 may be replaced by the expression $K_d KV$. Also, $SF^*(S) = 0$ for the condition of constant grinding force, the block diagram shown in Fig. 5 may be replaced by the diagram shown in Fig. 6.

The transfer function of this diagram may be shown to be

Fig. 5 Grinding system block diagram

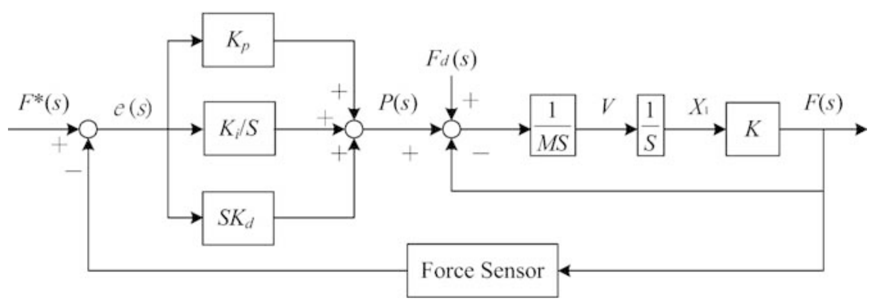

Fig. 6 Modified grinding system block diagram

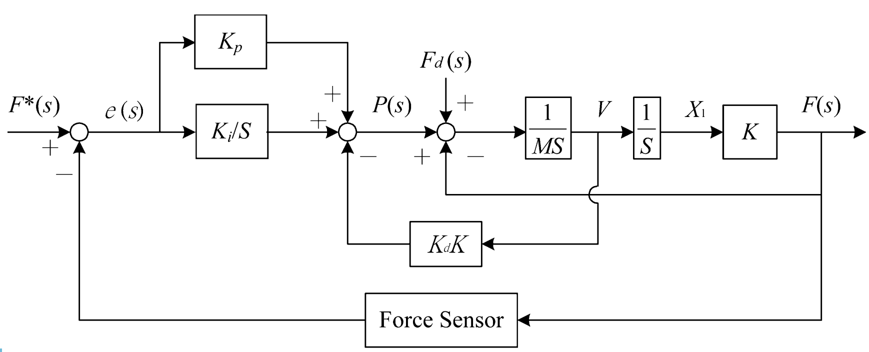

$$G(s)=\frac{F(s)}{F^{*}(s)}=\frac{K_pKs+K_iK}{Ms^3+K_dKs^2+\left(K_pK+K\right)s+K_iK} \tag{13}$$

The numerator polynomial in the current transfer function is one degree less than the transfer function defined by Eq. 9, which means the current transfer function has less zero point and also less influence upon a pole. Also, in the block diagram of Fig. 5 the error $e(s)$ is differentiated once, implying that the induced noise will be amplified, and this does not happen in the current block diagram. Therefore in the following discussion, the block diagram shown in Fig. 6 is used.

In order to determine controller gains, the first obvious point is that the denominator of Eq. 13 is a polynomial of the third order, and can be written in the form

$$\begin{aligned} g(S) &\equiv MS^3+K_dKS^2+\left(K_pK+K\right)S+K_iK \\ &=(S+a)(S+\alpha+j\beta)(S+\alpha-j\beta) \end{aligned} \tag{14}$$

Since it is relatively difficult to analyse a third order system, the purpose now is to approximate this system with a second order one, by assuming the two complex roots are dominant roots. Requiring that percent overshoot of the second order system does not exceed 3%, the following relation may be obtained [21]

$$0.03=e^{-\pi\zeta\big/\sqrt{1-\zeta^2}} \tag{15}$$

which implies $\pi\zeta\big/\sqrt{1-\zeta^2}=3.057$, or $\zeta=0.75$. As the first attempt to determine system gains, settling time T_S is arbitrarily set to 0.5 s. This means [21]

$$T_S=\frac{4}{\zeta\omega_n}=0.5\ \mathrm{s} \tag{16}$$

thus $\zeta\omega_n=8$, and $\omega_n=10.67$ rad/s.

The angle θ (see Fig. 7) take the value $\cos^{-1}\zeta$ or 41.4°. Therefore the complex poles of the characteristic equation (i.e. the equation $g(S)=0$, see Eq. 14) are $S=-8\pm j7.05$. The idea is to keep the third pole away from these two complex poles. The value $S=-15$ is arbitrarily chosen, hence Eq. 14 can be written in the form

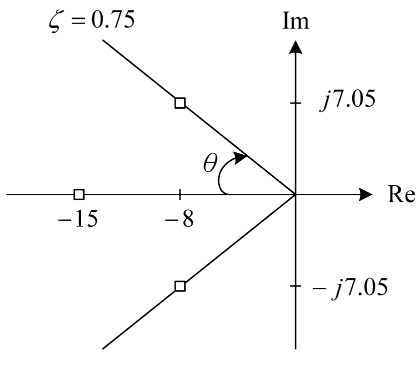

Fig. 7 Root locus of the characteristic equation

$$g(S)=S^3+31S^2+353.7S+1705.5=0 \tag{17}$$

Comparing coefficients of the last equations to the denominator of Eq. 13, the following relations are obtained

$$\frac{K_dK}{M}=31 \tag{18a}$$

$$\frac{K_pK+K}{M}=353.7 \tag{18b}$$

and

$$\frac{K_iK}{M}=1705.5 \tag{18c}$$

The value of K is estimated in the appendix to be $K=8.74\times10^3$(N/m), and mass of the hand grinder (with holder and link) is $M=5$ kg, substituting these values into Eqs. 18a, 18b, 18c, $K_d=0.0178$, $K_d=-0.797$, and $K_i=0.98$ may be obtained. Since system gains cannot be negative, a second trial, with new values of settling time T_s and natural frequency ω_n, is necessary.

For the second trial, the settling time is assumed to be 0.25 s, i.e. $T_S=4/(\zeta\omega_n)=0.25$ swhich means $\omega_n=21.3$, and $\zeta\omega_n=16$. Following the same steps as in the first trial, the two complex poles may be determined to be $S=-16\pm j14.1$. Now assuming that the third pole is at the point $S=-45$, then the characteristic equation is

$$S^3+77S^2+1895S+20466=0 \tag{19}$$

and after comparing corresponding coefficients, one finds

$$\frac{K_dK}{M}=77 \tag{20a}$$

$$\frac{K_pK+K}{M}=1895 \tag{20b}$$

and

$$\frac{K_iK}{M}=20466 \tag{20c}$$

which means $K_d=0.0443$, $K_P=0.0891$, and $K_i=11.762$.

The zero of the system is the root of the equation in the numerator of Eq. 13, i.e. the equation

$$K_pKS+K_iK=0 \tag{21}$$

Substituting the above values into this equation, one may find that the zero is the point $S=-132.0$. Hence the transfer function defined by Eq. 13 may be written in the form

$$\begin{aligned} G(S)=\frac{F(S)}{F^{*}(S)} &=\frac{\left(K_pK\big/M\right)(S+K_i/K_PM)}{S^3+77S^2+1895S+20466} \\ &=\frac{155.034(S+132)}{(S+45)(S+16+j14.1)(S+16-j14.1)} \end{aligned} \tag{22}$$

Note that in steady state, $G(S)$ approaches 1 as $S\rightarrow0$.

4 Simulation results and discussions

The system response may be obtained using the commercial software Matlab. In the simulation procedure, the spring constant $K = 8.74\times10^3$(N/m), mass of the hand grinder (with holder and link) $M = 5$ kg, system gains are $K_d = 0.004$, $K_p = 0.089$ and $K_i = 11.762$. The sampling time is chosen to be 0.001 s.

The loop transfer function of block diagram shown in Fig. 6 is

$$L(S) = \frac{K_pKS + K_iK}{Ms^3 + K_dKS^2 + KS} \tag{23}$$

With the system gains just obtained, the root-locus diagram corresponding to loop transfer function 23 may be drawn and is shown in Fig. 8. The three poles of Eq. 22 are shown in this diagram. It can seen that both the zero and the third pole are much farther apart from the imaginary axis than the dominant complex roots, making them have negligible influence on the system, hence the system may be approximated by a second order one.

With the gain values just obtained, the Bode diagram for the transfer function $G(s)$ defined by Eq. 13 is drawn (the Bode diagram of the process model without controllers is given in Fig. 9) and is shown in Fig. 10. Comparing this diagram to the Bode diagram of the process model without controllers, (i.e. Fig. 9) one may find that the resonance has been greatly reduced. Also, while the phase margin shown in Fig. 9 is approximately 180°, which corresponds to an unstable state, the phase angle shown in Fig. 10 is approximately 45°.

Due to the fact that the grinding force control system takes step input, step responses for the grinding process with and without controller are compared. Figure 11 shows step responses without controller, and Fig. 12 shows step response with the controller just designed has

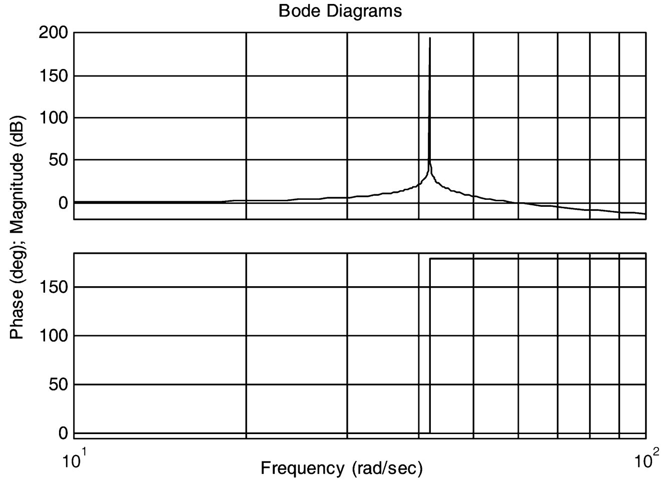

Fig. 9 Bode diagram of the grinding process

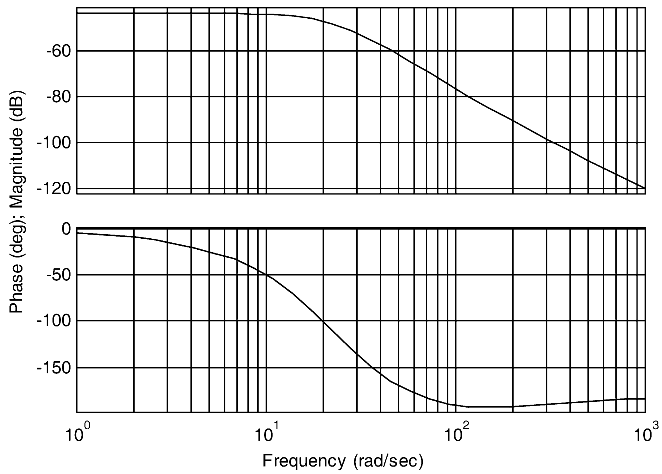

Fig. 10 Bode diagram of the grinding process with controller

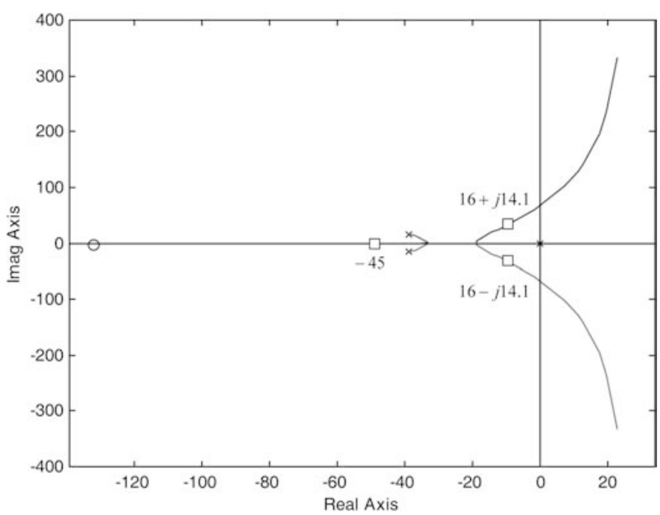

Fig. 8 Root-locus diagram of open loop system

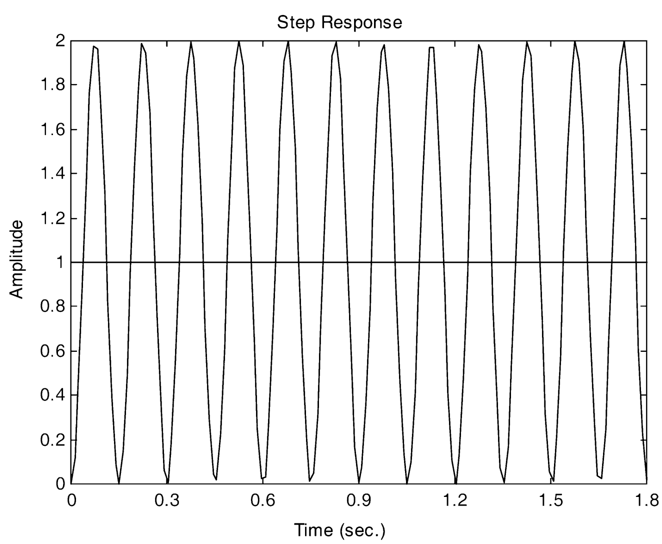

Fig. 11 Step response of the grinding process

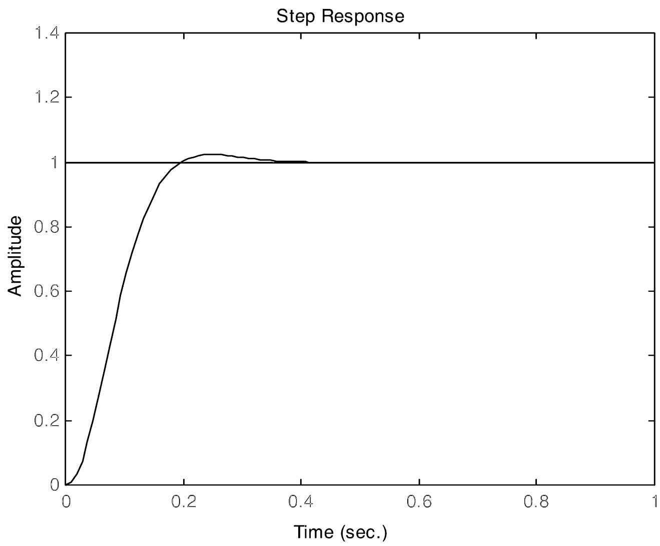

Fig. 12 Step response of the grinding process with controller

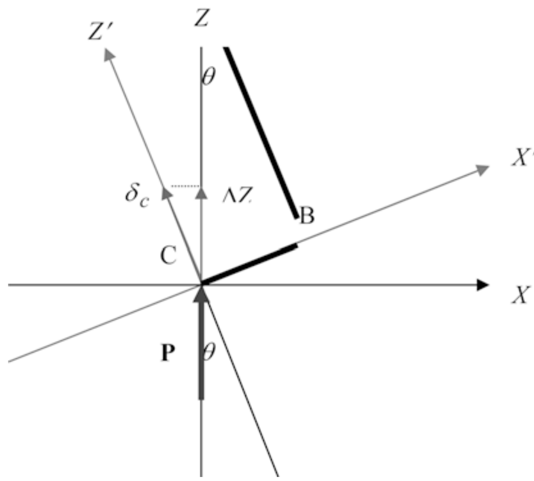

Fig. 13 Simplified model of hand grinder (with holder) for calculating k_1

been imposed. In the system without controller, grinding force oscillates with no steady state and in the system with force control; the settling time is less than 0.25 s with a percent overshoot of less than 3%. These system gains (i.e. $K_d = 0.044$, $K_P = 0.089$, and $K_i = 11.762$), have been utilised in the automatic grinding system with force control; results show that surface roughness may be reduced [9].

5 Conclusions

In this study, a grinding process model for the force control system utilises a CNC machine centre, an electric hand grinder and a force sensor has been proposed. This force control system is represented by a spring-mass system and according to estimated stiffness of each component, the spring-mass system may be further simplified. A PID controller base on the simplified system has been designed. Controller gains are estimated by using the commercial software Matlab. Estimation results show that a settling time of less than 0.25 s and a percent overshoot of less than 3% may be obtained.

Acknowledgements The authors gratefully acknowledge that this study was supported by the National Science Council of ROC under grant no. NSC 89-2218-E032–030.

Appendix: Estimations of stiffness constants

Stiffness of hand grinder (with link and holder): k_1

In Fig. 13, segment *AB* represents the link (see Fig. 1) which has a length *a* and makes an angle θ with the *Z*-axis. The electric hand grinder is presented by segment *BC* which is normal to segment *AB* and the length of which is *b*. As the normal grinding force *P* is applied, the corresponding displacement of member *ABC* (*i.e.* the combined parts of link, holder, and hand grinder) at the point *C* is ΔZ, which is to be estimated in two steps. First, segment *AB* is tightly fixed to the spindle and may be represented by a cantilever beam, as shown in Fig. 14. The angle at point *B* due to the force $P\sin\theta$ and the moment $Pb\cos\theta$ is

$$\theta_b = \frac{Pba\cos\theta}{E_a I_a} - \frac{Pa^2\sin\theta}{2E_a I_a} \tag{24}$$

where E_a and I_a are modulus of elasticity and area moment of inertia of the segment *AB*, respectively. Secondly, segment *BC* is also modelled by a cantilever beam but it has an initial inclination angle θ_b, as shown in Fig. 15. The deflection at *C* of this beam due to the load is given by

$$CC' = \frac{Pb^3\cos\theta}{3E_b I_b} \tag{25}$$

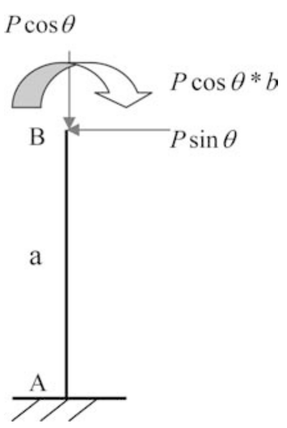

Fig. 14 Link *AB* is modelled by a cantilever beam

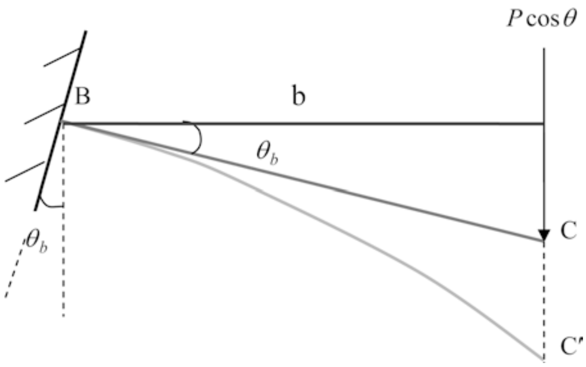

Fig. 15 Link BC is also modelled by a cantilever beam

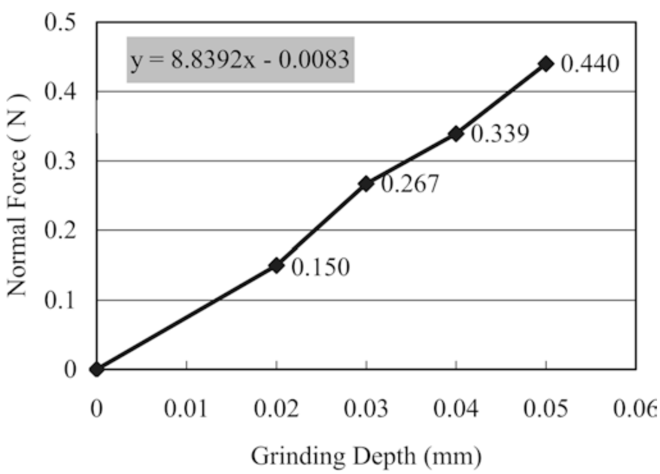

Fig. 16 Normal force versus grinding depth (tool diameter is 9.5 mm, feed rate = 20 mm/min, and rotation speed = 20,000 rpm)

where E_b and I_b denote modulus of elasticity and area moment of inertia of the segment BC respectively. The total displacement at C in the direction of Z' may be approximated by the relation

$$\delta_c = CC' + b\theta_b = \frac{Pb^3 \cos\theta}{3E_b I_b} + \frac{Pab(2b\cos\theta - a\sin\theta)}{2E_a I_a} \tag{26}$$

and thus the displacement at C in the Z direction is

$$\Delta Z = \delta_c \cos\theta = \frac{Pb^3 \cos^2\theta}{3E_b I_b} + \frac{Pab\cos\theta(2b\cos\theta - a\sin\theta)}{2E_a I_a} \tag{27}$$

Link AB is made of stainless steel with the modulus of elasticity $E_a = 210$ GPa. The hand grinder is a combination of stainless steel and aluminum alloy. The value $E_b = 70$ GPa is used and later one will see that any value between 70 Gpa (aluminum) and 210 GPa (steel) may also be used and has very little effect on the final result. Diameters of segment AB and BC are $d_a = 0.036$ m and $d_b = 0.026$ m respectively. Using the relation $I = \pi d^4/64$, one may determine $I_a = 8.2 \times 10^{-8}$ m and $I_b = 2.2 \times 10^{-8}$ m respectively. Substituting these values, together with the lengths $a = 0.13$ m, $b = 0.195$ m and the angle $\theta = 30°$ into Eq. 27 one may obtain $Z = 1.38 \times 10^{-6} P$. Then the stiffness of the first spring is $k_1 = P/\Delta Z = 7.25 \times 10^5$ N/m.

Stiffness of material removal process: k_2

Grinding force for a certain grinding depth may be obtained by using the force sensor shown in Fig. 1 (Kistler_5295A). As feed rate is 20 mm/min, rotation speed is 20,000 rpm, and tool diameter is 9.5 mm, normal grinding forces are measured with various grinding depths. Average grinding forces versus grinding depths are plotted in Fig. 16. The relation is roughly linear and the slope is taken to be the stiffness k_2, hence approximately $k_2 = 8.84 \times 10^3$ N/m.

Stiffness of work-piece: k_3

Stiffness of the work-piece may be estimated by using the finite element method. For example, specimens used by Chen [9] have the size 40mm × 40mm × 15 mm, and are made of SKD61 steel. Using the commercial software I-DEAS version 7.0, the displacement at the centre as a force 100 N is applied is calculated to be 1.5×10^{-7} m. Hence the stiffness $k_3 = 6.67 \times 10^8$ N/m.

Equivalent stiffness K for the series of springs k_1, k_2, and k_3

The equivalent stiffness K is given by

$$\frac{1}{K} = \frac{1}{k_1} + \frac{1}{k_2} + \frac{1}{k_3} \tag{28}$$

Substituting values of k_1,k_2, and k_3 into Eq. 28, it is found that $K = 8.74 \times 10^3$ N/m. One may notice that both k_1, and k_3 are much larger than k_2, hence the right-hand side of Eq. 28 and also the equivalent stiffness K, are dominated by k_2.

Stiffness of the force sensor: k_4

The operation manual of the force sensor (Kistler_5295A) gives the value $k_4 = 2.6 \times 10^9$ N/m.

References

1. Hahn RS (1964) Controlled-force grinding—a new technique for precision internal grinding. J Eng Ind 86:287–293
2. Shaw MC (1996) Principles of abrasive processing. Oxford University Press, Oxford

3. Liu L, Ulrich BJ, Elbestawi MA (1990) Robotic grinding force regulation: design, implementation and benefits. In: Proceedings of the 1990 IEEE international conference on robotics and automation, pp 258–265
4. Jenkins HE, Kurfess TR (1995) Adaptive pole-zero cancellation in grinding force control. IEEE Trans Contr Syst Tech 7:363–370
5. Jenkins HE, Kurfess TR (1999) Adaptive process estimation for a grinding system. In: Proceeding of the ASME dynamic system and control division 57:483–489
6. Jenkins HE (1996) Process estimation and adaptive control of grinding system. PhD thesis, Georgia Institute of Technology
7. Chen CHA, Duffie NA (1996) Development of an automatic surface finishing system (ASFS) with in-process surface topography inspection. J Mater Process Tech 62:427–430
8. Hsu TC (1998) Automatic surface finishing with rough area pattern recognition. PhD thesis, University of Wisconsin-Madison
9. Chen JC (2000) Force control in grinding processes. Masters thesis, Tamkang University
10. Tönshoff HK, Peters J, Inasaki I, Paul T (1992) Modeling and simulation of grinding processes. Ann CIRP 41:677–688
11. Ludwick SJ, Jenkins HE, Kurfess TR (1994) Determination of dynamic grinding model. Trans ASME Dyn Syst Contr 55:843–849
12. Jenkins HE, Kurfess TR (1996) Optimization of real-time multivariable estimation in grinding. Trans ASME Dyn Syst Contr 58:365–370
13. Hahn RS, Lindsay RP (1971) Principles of grinding, part 1: basic relationships in precision machining. Machinery, pp 55–62
14. Brown N (1990) Optical fabrication, MISC4476, revision 1. Lawrence Livermore, Livermore
15. Jenkins HE, Kurfess TR (1997) Dynamic stiffness implications for a multiaxis grinding system. J Vib Cont 3:297–313
16. Hekman KA, Liang SY (1999) Feed rate optimization and depth of cut control for productivity and part parallelism in grinding. Mechatronics 9:447–462
17. Kurfess TR, Whitney DE, Brown ML (1988) Verification of a dynamic grinding model. Trans ASME J Dyn Syst Meas Contr 110:403–409
18. Whitney DE, Edsall AC, Todtenkopf AB, Kurfess TR, Tate AR (1990) Development and control of an automatic robotic weld bead grinding system. Trans ASME J Dyn Syst Meas Contr 112:166–176
19. Kurfess TR, Whitney DE (1992) Predictive control of a robotic grinding system. Trans ASME J Eng Ind 114:412–420
20. Lin C (1999) Three-dimensional grinding force measurement in mold grinding processes. Masters thesis, Tamkang University (in Chinese)
21. Kuo BC (1995) Automatic control systems, 7th edn. Prentice-Hall, New York